Springer

KSME

Journal of Mechanical Science and Technology 26 (9) (2012) 2913~2919
www.springerlink.com/content/1738-494x
DOI 10.1007/s12206-012-0709-8

A 2-dof gravity compensator with bevel gears †

Changhyun Cho[1], Woosub Lee[2,3], Jinyi Lee[1] and Sungchul Kang[2,*]

[1]*Department of Control, Instrument and Robot, Chosun University, Gwang-ju, 501-759, Korea*
[2]*Center for Bionics, Korea Institute of Science and Technology (KIST), Seoul, 136-791, Korea*
[3]*Department of Mechanical and Aerospace Engineering, Tokyo Institute of Technology, Tokyo, 152-8552, Japan*

(Manuscript Received June 13, 2011; Revised January 29, 2012; Accepted March 18, 2012)

Abstract

This paper presents a 2-dof gravity compensator used for roll-pitch rotations, which are often applied to the shoulder joint of a service or humanoid robot. The 2-dof gravity compensator is comprised of two 1-dof gravity compensators and a bevel differential. The roll-pitch rotations are decoupled into two rotations on the moving link by the bevel differential; the two 1-dof gravity compensators are applied to the two rotations. The spring coefficients are determined through energy and torque analyses in order to achieve complete static balancing. The experiment results indicate that the proposed gravity compensator effectively counterbalances the gravitational torques and can also be operated in the hemispherical work space.

Keywords: Bevel gears; Gravity compensation; Manipulator; Static balancing

1. Introduction

Service robot manipulators are often required to operate in relatively large workspaces and are may be operated at low velocities for safety reasons. In such cases the gravitational or static torques become more of a consideration than the dynamic ones. To overcome the inefficiencies inherent to static torques, gravity compensators have been developed to counterbalance the gravitational torques generated by the manipulator mass [1]. Complete gravity compensation is defined as when the link masses no longer generate any torque at the joints in all manipulator configurations.

Gravity compensators using a variety of springs have been proposed over the last three decades [2]. A 1-dof static balancer with a single spring has been proposed in Ref. [3]. A 1-dof gravity compensator comprised of a pulley, wire and spring was presented by Ulrich and Kumar in 1991 [4]. An internal cam device used to counterbalance the gravitational torque has been developed and applied to a 3-dof 5-bar mechanism [5]. In 2003 Morita et al. presented a 3-dof gravity compensator used for yaw-roll-pitch rotations employing a single spring [6]. A design method using an *n*-spring balancer for a one-link system with a 2-dof rotation was developed based on potential energy by Walsh et al. in 1991 [7].

For a multi-link manipulator, the COM (center of mass) of the distal link with respect to the inertial frame varies with the rotation of the proximal link. To overcome this limitation caused by these complex rotations, a parallel constraint is often applied to the distal link to deliver the rotation of the distal link to the base link [3, 6, 8, 9]. Parallelograms [3] and pseudo parallelograms [6, 8] have been suggested for this purpose. The rotation of the distal link can be delivered to the base link with a parallelogram where a 2-dof gravity compensator is attached [9]. Agrawal and Fattah proposed a hybrid strategy for an n-link manipulator [10]. In their research a parallelogram was adopted to represent the COM; springs were applied to the parallelogram. Gravity-compensated parallel mechanisms have been designed that utilize the concepts of balance springs and counterweights [11, 12].

This paper presents a 2-dofs gravity compensator used for roll-pitch rotations. Roll-pitch rotations are often found in the shoulder joints of human-like service robots. The proximal link of a service robot often possesses an almost hemispherical workspace. Since a point regarding the proximal link only moves along the hemispherical surface in this situation, the hemispherical workspace does not indicate a hemispherical working volume. Therefore, a gravity compensator for a service robot needs to provide compensation for the particular hemispherical surface workspace under consideration. The proposed gravity compensator is comprised of two 1-dof gravity compensators and a bevel differential. One bevel gear is fixed at the base; the other bevel gears revolve around the fixed one and rotate on its axis. The roll-pitch rotations are decoupled into two bevel gear rotations on the moving link and the two 1-dof gravity compensators are attached to their

*Corresponding author. Tel.: +82 2 958 5589, Fax.: +82 2 958 5629
E-mail address: kasch804@gmail.com
† Recommended by Associate Editor Sangyoon Lee

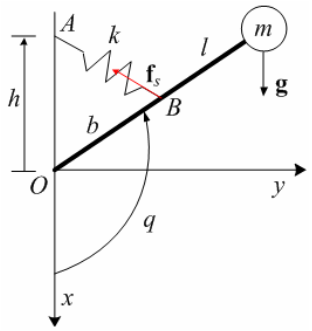

Fig. 1. The 1-link manipulator with roll-pitch rotations.

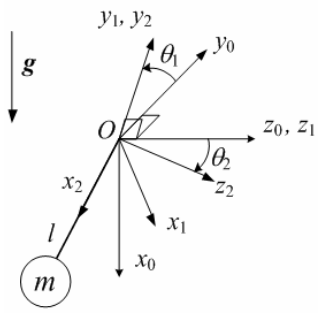

Fig. 2. The 1-dof gravity compensator.

respective rotating bevel gears to achieve the hemispherical work space. To determine the spring coefficients the total potential energy of the springs and the manipulator mass is investigated as described in Refs. [6-8, 10]. The energy analyses reveal that the proposed compensator can deliver complete static balancing. The gravity compensation experiment results demonstrate that the proposed compensator can effectively counterbalance the gravitational torques and can operate in a hemispherical workspace. Note that the bevel gravity compensator was briefly introduced with preliminary experiments [13, 14]. Also note that the proposed 2-dof gravity compensator only works when the mass center is fixed. In a two-link manipulator, however, the mass center varies due to the rotation of the distal link. To overcome this limitation a counter mass is applied to the distal link [13] and spring balancers are used at the elbow joint [14].

The rest of this paper is organized as follows: Section 2 presents the 1-link manipulator with its roll-pitch rotations, Section 3 introduces the 1-dof gravity compensator and the bevel gravity compensator, Section 4 discusses the gravity compensation experiment results, and finally Section 5 provides our conclusions.

2. The 1-link manipulator with roll-pitch rotations

A schematic of the 1-link manipulator is shown in Fig. 1. θ_1 and θ_2 represent the rotation angles in the z_0 and in the y_1 directions, respectively. In this situation the rotation matrix for Fig. 2 is computed using:

$$ {}^0\mathbf{R}_2 = \mathbf{R}_z(\theta_1)\mathbf{R}_y(\theta_2) . \tag{1} $$

The mass of the arm, m, is located at distance l from the origin. Let ${}^2\mathbf{p}$ and ${}^0\mathbf{p}$ be the position vectors of the COM with respect to the {2} and {0} frames, respectively. ${}^0\mathbf{p}$ is determined by ${}^0\mathbf{p} = {}^0\mathbf{R}_2{}^2\mathbf{p} = l[c_1c_2, s_1c_2, -s_2]^T$, where ${}^2\mathbf{p} = [l, 0, 0]^T$. Note that c_i and s_i represent $\cos\theta_i$ and $\sin\theta_i$.

The gravitational torques can be computed by the principle of the virtual work. Suppose that gravity is applied in the positive x direction. The gravitational torque $\boldsymbol{\tau}_m$ is determined by:

$$ \boldsymbol{\tau}_m = {}^0\mathbf{J}_P^T[mg,0,0]^T = -mgl[s_1c_2, c_1s_2]^T \tag{2} $$

where ${}^0\mathbf{J}_p = l[-s_1c_2, -c_1s_2; c_1c_2, -s_1s_2; 0, -c_2] \in R^{3\times2}$ and $\boldsymbol{\tau}_m = [\boldsymbol{\tau}_{m1}, \boldsymbol{\tau}_{m2}]^T$) (= $\boldsymbol{\tau}_{m1}\mathbf{a}_{z0} + \boldsymbol{\tau}_{m2}\mathbf{a}_{y1}$, where $\mathbf{a}_{zi}$ represents the unit vector in the z_i direction). g denotes the gravitational acceleration. The potential energy of the manipulator mass by the gravity is computed by:

$$ V_m(\theta_1,\theta_2) = -{}^0\mathbf{p}\cdot mg\mathbf{a}_x = -mglc_1c_2 . \tag{3} $$

3. The bevel gravity compensator

The bevel gravity compensator is addressed in this section. The 1-dof gravity compensator used in the bevel gravity compensator is briefly described and the bevel differential motions are discussed. It is demonstrated from the motions of the bevel differential that the roll-pitch rotations are decoupled into two rotations with respect to the moving link. The spring coefficients are determined by energy and torques analyses in order to attain complete gravity compensation.

3.1 The 1-dof gravity compensator

The 1-dof gravity compensator used in the bevel gravity compensator is summarized in Refs. [3, 6, 7] and illustrated in Fig. 2. One spring end is attached to point A fixed at ground and the other is attached to point B located at the arm. Points A and B are located at distances h and b from the origin O, respectively. A zero-length spring is used, which has zero length at zero deflection (e.g., the initial state). The mass of m is located at distance l from the origin. For the practical implementation of the zero-length spring, the section between points A and B can be interconnected with a wire; the spring is attached to the base or the arm. The spring coefficient that gives complete gravity compensation is computed based on the torque [3, 4] and the energy [6, 7].

Suppose that the torque caused by the gravity is completely canceled by the torque generated by a spring as shown in Fig. 2. In this situation the total torque at the origin is computed by:

$$ \boldsymbol{\tau}_0 = \mathbf{r}_B \times \mathbf{f}_s + \mathbf{r}_m \times m\mathbf{g} = \mathbf{0} \tag{4} $$

where $\mathbf{r}_i$ denotes the position vector of point i and $\mathbf{f}_s$ represents the force vector generated by the spring. $\mathbf{r}_B = b[\cos q, \sin q, 0]^T$, $\mathbf{r}_m = l[\cos q, \sin q, 0]^T$ and $\mathbf{0} = [0, 0, 0]^T$. Assume that the gravity is applied in the positive x direction (i.e., $\mathbf{g} = [g, 0, 0]$). Since a zero length spring is used, $\mathbf{f}_s$ is derived by:

$$\mathbf{f}_s = k\mathbf{r}_{AB} = k(\mathbf{r}_A - \mathbf{r}_B) \tag{5}$$

where k represents the spring coefficient and $\mathbf{r}_A = [-h, 0, 0]^T$. Therefore, Eq. (4) becomes:

$$\boldsymbol{\tau}_0 = (bhk - mgl)\sin q\,\mathbf{a}_z = \mathbf{0} \tag{6}$$

where $\mathbf{a}_z$ denotes the unit vector in the z direction. To satisfy Eq. (6) for all q, $(bhk - mgl)$ needs to be zero. Therefore, the spring coefficient is determined using:

$$k = mgl / bh\,. \tag{7}$$

In this manner, complete gravity compensation is achieved using $k = mgl/bh$ for the 1-dof gravity compensator.

Consider the total potential energy of the spring and the manipulator mass. Let V_k and V_m be the potential energy of the spring and the manipulator mass, respectively. The total potential energy needs to be invariant to achieve complete gravity compensation [7]:

$$V = V_m + V_k = const. \tag{8}$$

where $V_m = -\mathbf{r}_m \cdot m\mathbf{g}$ and $V_k = k|\mathbf{r}_{AB}|^2/2$. From Fig. 2, $|\mathbf{r}_{AB}|^2 = b^2 + h^2 + 2bh\cos q$ and $-\mathbf{r}_m \cdot m\mathbf{g} = -mgl\cos q$. Therefore, Eq. (8) is rewritten as:

$$V = k(b^2 + h^2)/2 + (bhk - mgl)\cos q = const\,. \tag{9}$$

The partial differential of Eq. (9) is computed using:

$$\partial V / \partial q = (mgl - bhk)\sin q = 0\,. \tag{10}$$

To satisfy Eq. (10) for all q, $(mgl - bhk)$ needs to be set to zero and, therefore, the same result (i.e., Eq. (7)) is obtained. Note that the 1-dof gravity compensator can be operated over the full range of q (i.e., $-\pi \le q \le \pi$), since the 1-dof gravity compensator has symmetry along the x-axis.

3.2 The bevel gravity compensator

Schematics of the bevel gravity compensator are presented in Fig. 3. The pose of $\theta_1 = 0$ and $\theta_2 = -\pi/2$ is illustrated in Fig. 3(a). The bevel differential is located inside link 1 which rotates in the z_0 direction (i.e., θ_1). One bevel gear is fixed at the base in the z_0 direction and the others revolve around the fixed bevel gear and rotate on its axis. The rotating bevel gears and link 2 are attached to the y_1 axis and rotate freely in the y_1 direction. Therefore, link 1 and link 2 rotate along the fixed bevel gear and rotating bevel gears, respectively.

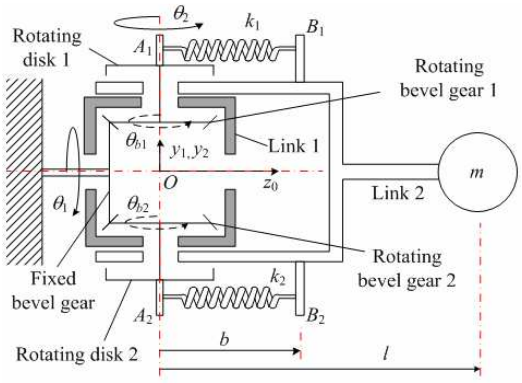

(a) Locations of the 1-dof gravity compensator

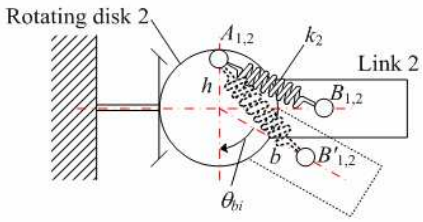

(b) Rotation in the y_1 direction

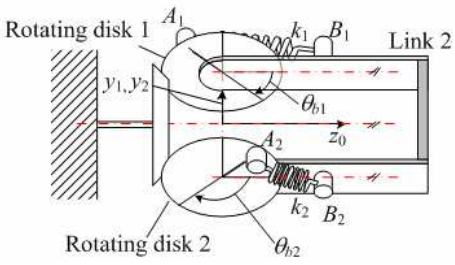

(c) Rotation in the z_0 direction

Fig. 3. The bevel gravity compensator schematics.

Let θ_{b1} and θ_{b2} be the angles of the rotating bevel gears with respect to link 2 along the y_2 axis. Consider the motion of the bevel gears. When link 1 is fixed and link 2 rotates in the positive y_1 direction (i.e., downward) as shown in Fig. 3(b), θ_{b1} and θ_{b2} rotate in the negative y_2 direction with respect to link 2. When link 1 rotates in the positive z_0 direction (i.e., θ_1) and link 2 is fixed as shown in Fig. 3(c), θ_{b1} and θ_{b2} rotate in the negative y_2 direction and in the positive y_2 direction, respectively. Assume that reduction ratios of 1:1 are applied to the bevel differential and $\theta_{bi} = 0$ for all i, when $\theta_1 = \theta_2 = 0$. Let $\boldsymbol{\theta} = [\theta_1, \theta_2]^T$ $(= \theta_1\mathbf{a}_{z0} + \theta_2\mathbf{a}_{y1})$ and $\boldsymbol{\theta}_b = [\theta_{b1}, \theta_{b2}]^T$ $(= \theta_{b1}\mathbf{a}_{y2} + \theta_{b2}\mathbf{a}_{y2})$. $\boldsymbol{\theta}_b$ is computed using:

$$\boldsymbol{\theta}_b = {}^2\mathbf{J}\boldsymbol{\theta} \tag{11}$$

where ${}^2\mathbf{J} = [-1, -1; 1, -1] \in R^{2\times 2}$. Therefore, the roll-pitch rotations are decoupled into θ_{b1} and θ_{b2} with respect to link 2, whereas θ_1 and θ_2 are determined with respect to link 1 and

link 2, respectively. Note that the fixed bevel gear can be located at the opposite position (i.e., far from the base, as seen in Fig. 3(a)). In this situation θ_{b1} and θ_{b2} rotate in the positive y_2 direction and in the negative y_2 direction for the rotation of θ_1 and so ${}^2\mathbf{J} = [1, -1; -1, -1]$.

Rotating disks 1 and 2 are attached outside of link 2 and fixed at the rotating bevel gears. Therefore, the angles of the rotating disks are identical to $\boldsymbol{\theta}_b$. Points A_i and B_i are located at rotating disk i and link 2, respectively. Point A_i is located at distance h from the origin and the angle of $\theta_{bi} + \pi$. Point B_i is located at distance b from the origin. Note that points A_i and B_i in Fig. 3(a) represent the same points found in Fig. 2. Zero length springs k_1 and k_2 are attached between points A_1 and B_1, and A_2 and B_2, respectively. Thus, two 1-dof gravity compensators are applied to their respective rotating disks. For the 1-dof gravity compensator in Fig. 2 one end of the spring is affixed to the base, whereas the bevel gravity compensator shown in Fig. 3(a) is attached to the rotating disk, which rotates correspondingly to the pose of the manipulator (i.e., the variances of θ_1 and θ_2 from Eq. (11)).

Rotation in the y_1 direction (i.e., θ_2) is depicted in Fig. 3(b). In this situation no rotation occurs for the rotating disk and therefore points A_1 and A_2 are fixed. As link 2 rotates, points B_1 and B_2 move to points B_1' and B_2', thereby resulting in an extension of the springs. θ_{b1} and θ_{b2} decrease in the y_2 direction with respect to link 2, as denoted in Eq. (11).

Consider rotation in the z_0 direction (i.e., θ_1) as shown in Fig. 3(c). In this situation points A_1 and A_2 rotate in the negative y_2 direction and in the positive y_2 direction, respectively, whereas B_1 and B_2 maintain their positions at the parallel line of z_0. In Eq. (11), θ_{b1} decreases and θ_{b2} increases as link 2 rotates in the positive z_0 direction. Therefore, the deflection of k_1 increases and that of k_2 decreases, since point A_i is attached to $\theta_{bi} + \pi$.

The potential energy of the springs can be investigated. The position of A_i with respect to link 2 is determined by:

$$ {}^2\mathbf{p}_{Ai} = h[\cos(\theta_{bi} + \pi), \sin(\theta_{bi} + \pi), 0]^T = -h[\cos\theta_{bi}, \sin\theta_{bi}, 0]^T \tag{12} $$

for all i. The position of B_i with respect to link 2 is ${}^2\mathbf{p}_{Bi} = [b, 0, 0]^T$. Assuming that zero length springs are utilized, the deflection of spring k_i is computed using:

$$ s_i^2 = |\, {}^2\mathbf{p}_{Ai} - {}^2\mathbf{p}_{Bi} \,|^2 = b^2 + h^2 + 2bh\cos\theta_{bi} \,. \tag{13} $$

From Eq. (11), Eq. (13) can be rewritten as:

$$ s_i^2 = b^2 + h^2 + 2bh\cos({}^2\mathbf{J}_i\boldsymbol{\theta}) \tag{14} $$

where ${}^2\mathbf{J}_i$ denotes the i-th row vector of ${}^2\mathbf{J}$ in Eq. (11). Since two springs are utilized in the bevel gravity compensator, the total potential energy of the springs is determined by:

$$ V_k = (k_1 s_1^2 + k_2 s_2^2)/2 \,. \tag{15} $$

Substituting Eq. (14) into Eq. (15) yields:

$$ V_k = C + bhk(\cos(\theta_1 + \theta_2) + \cos(\theta_1 - \theta_2)) \,. \tag{16} $$

By considering the symmetry of the springs along the x_2 axis, we can set $k_1 = k_2 = k$. With the value ${}^2\mathbf{J}$ from Eq. (11), Eq. (16) becomes:

$$ V_k = C + bhk(\cos(\theta_1 + \theta_2) + \cos(\theta_1 - \theta_2)) \tag{17} $$

where $C = 2k(b^2 + h^2)$. Since $\cos(\theta_1 + \theta_2) + \cos(\theta_1 - \theta_2) = 2c_1c_2$, the potential energy of the springs is finally computed by:

$$ V_k = C + 2bhkc_1c_2 \,. \tag{18} $$

The same results found for Eq. (18) can be obtained for ${}^2\mathbf{J} = [1, -1; -1, -1]$ (i.e., the fixed bevel gear is located at the opposite position).

The total potential energy of the springs and the manipulator mass remain constant to achieve complete gravity compensation, similar to that found in Eq. (8). Using Eqs. (3) and (18), the total potential energy of the springs and the manipulator mass is derived by $V = V_m + V_k = const$. The partial differential of V is determined by:

$$ \partial V / \partial\theta_i = \partial V_m / \partial\theta_i + \partial V_k / \partial\theta_i = 0. \tag{19} $$

From Eq. (3) $\partial V_m/\partial\theta_i$ is computed using:

$$ \partial V_m / \partial\theta_1 = mgls_1c_2, \partial V_m / \partial\theta_2 = mglc_1s_2 \,. \tag{20} $$

From Eq. (18) $\partial V_k/\partial\theta_i$ is determined by:

$$ \partial V_k / \partial\theta_1 = -2bhks_1c_2, \partial V_k / \partial\theta_2 = -2bhkc_1s_2 \,. \tag{21} $$

Substituting Eqs. (20) and (21) into Eq. (19) yields:

$$ (mgl - 2bhk)[s_1c_2, c_1s_2]^T = \mathbf{0} \,. \tag{22} $$

Eq. (22) is satisfied for all θ_i, when $mgl - 2bhk = 0$. The spring coefficient k is determined by:

$$ k = mgl / 2bh \,. \tag{23} $$

Recalling that $k = mgl/bh$ from Eq. (7) for the 1-dof gravity compensator, half of the stiffness is necessary for the bevel gravity compensator. This means a weaker spring can be applied to the bevel gravity compensator. Considering the spring number (i.e., two springs), however, the total stiffness of the springs has the same value as that found for the 1-dof gravity compensator.

The coefficient of the spring can be also determined through torque analyses. The torques at the θ_1 and θ_2 joints generated by the springs ($\tau_s = [\tau_{s1}, \tau_{s2}]^T$ (= $\tau_{s1}\mathbf{a}_{z0} + \tau_{s2}\mathbf{a}_{y1}$)) can be computed by the principal of the virtual work as in $\boldsymbol{\tau}_s = {}^2\mathbf{J}^T\boldsymbol{\tau}_b$,

where $\boldsymbol{\tau}_b = [\tau_{b1}, \tau_{b2}]^T$ (= $\tau_{b1}\mathbf{a}_{y2} + \tau_{b2}\mathbf{a}_{y2}$) and $\boldsymbol{\tau}_{bi}$ denotes the exerting torque at the rotating disk i by the spring k_i. Utilizing Eq. (4), τ_{bi} is computed by:

$$\begin{aligned}\tau_{bi} &= {}^2\mathbf{p}_{Ai} \times {}^2\mathbf{f}_{si} = {}^2\mathbf{p}_{Ai} \times k_i({}^2\mathbf{p}_{Bi} - {}^2\mathbf{p}_{Ai}) \\ &= k_i\, {}^2\mathbf{p}_{Ai} \times {}^2\mathbf{p}_{Bi} = k_i bh \sin\theta_{bi} .\end{aligned} \tag{24}$$

Taking into consideration the symmetry of the springs along the x_2 axis, we can state $k_1 = k_2 = k$. Therefore, straightforward computations of $\boldsymbol{\tau}_s = {}^2\mathbf{J}^T\boldsymbol{\tau}_b$ yield:

$$\boldsymbol{\tau}_s = \mathbf{J}^T\boldsymbol{\tau}_b = -kbh[\sin\theta_{b1} - \sin\theta_{b2}, \sin\theta_{b1} + \sin\theta_{b2}]^T . \tag{25}$$

Since θ_{b1} = -θ_1 - θ_2 and θ_{b2} = θ_1 - θ_2 from ${}^2\mathbf{J}$ in Eq. (11), Eq. (25) can be rewritten as:

$$\boldsymbol{\tau}_s = kbh[\sin(\theta_1+\theta_2) + \sin(\theta_1-\theta_2), \sin(\theta_1+\theta_2) - \sin(\theta_1-\theta_2)]^T . \tag{26}$$

Substituting $\sin(\theta_1 + \theta_2) + \sin(\theta_1 - \theta_2) = 2s_1c_2$ and $\sin(\theta_1 + \theta_2) - \sin(\theta_1 - \theta_2) = 2c_1s_2$ into (26) yields:

$$\boldsymbol{\tau}_s = 2kbh[s_1c_2, c_1s_2]^T . \tag{27}$$

The total moment at joint i needs to be zero for all θ_i to achieve complete gravity compensation. Using Eqs. (2) and (27), the total moment is determined by:

$$\boldsymbol{\tau}_m + \boldsymbol{\tau}_s = (2kbh - mgl)[s_1c_2, c_1s_2]^T = \mathbf{0} . \tag{28}$$

Eq. (28) has the value of zero for all θ_i, when $2kbh - mgl = 0$. Therefore, the same result is obtained as found in Eq. (23).

Since the 1-dof gravity compensator in Fig. 2 can be operated over the full range of q, as mentioned in Section 2, θ_{b1} and θ_{b2} rotate in the range of $-\pi \le \theta_{bi} \le \pi$ for all i. Therefore, θ_1 and θ_2 can also rotate in the range of $-\pi \le \theta_i \le \pi$ for all i, referring to Eq. (11). For practical implementation, however, the ranges of θ_1 and θ_2 are delimited to $-\pi \le \theta_1 \le \pi$ and $-\pi \le \theta_2 \le 0$ to avoid collisions with the base, thereby resulting in a hemispherical work space.

4. The experiments

4.1 The experiment setup

Pictures of the bevel gravity compensators are presented in Fig. 4. l and m have the values of 0.164 m and 6.7 kg, respectively. h_i and b_i are set to 0.0685 m and 0.049 m, respectively. The gravity is applied in the positive x_0 direction (i.e., ${}^0\mathbf{g} = [g, 0, 0]^T$). The spring coefficient is computed by $k = mgl/2bh$ = 1.59 kN/m. Two 50 W motors were implemented at the rotating bevel gears with the reduction ratio of 38:1. For this experiment setup the fixed bevel gear were located at the opposite side.

For these gravity compensation experiments, the host program in the PC sent the desired angles to the motor controllers and received the measured angles and motor currents from the motor controllers. The torques generated by the motors were obtained by multiplying the measured currents by the torque constants of the motors.

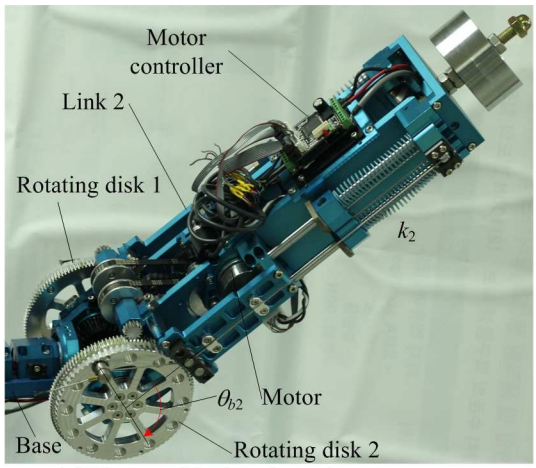

(a) Picture of the bevel gravity compensator

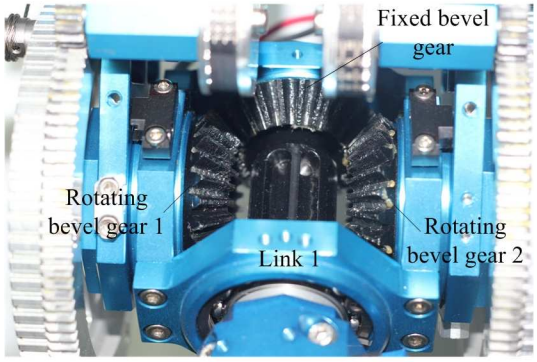

(b) Picture of the bevel gravity differential

Fig. 4. The bevel gravity compensator pictures.

4.2 The experiment results

Various poses from Table 1 were made to evaluate the gravity compensation performance. θ_1 and θ_2 were set to 0 and -π, respectively, for the initial pose (i.e., $t = 0$). That is, link 2 was fully raised in the negative x_0 direction. Each pose was maintained for 10s to achieve the static states (i.e., omega = 0 for all joints). Consider pose 1 for example. The rotation of θ_2 begins at t = 0s and holds until t = 10s after reaching θ_2 = -π/4. The gravity compensation experiments were conducted in half of the hemispherical work space, per Table 1. However, the performance of the bevel gravity compensator can be determined by the experiment results for half of the hemispherical work space because of its symmetrical nature.

The gravity compensation experiment results are presented in Figs. 5 and 6. The reference angle and omega in Figs. 5 and 6 denote θ_i from Table 1 and the measured angular velocity of θ_i. The gray areas in Figs. 5 and 6 represent the static situations. The measured motor torques are compared to the static

Table 1. The desired poses.

	θ_1 (rad)	θ_2 (rad)
Pose 1	0	$-\pi/4$
Pose 2	0	$-3\pi/4$
Pose 3	$\pi/4$	$-3\pi/4$
Pose 4	$3\pi/4$	$-3\pi/4$

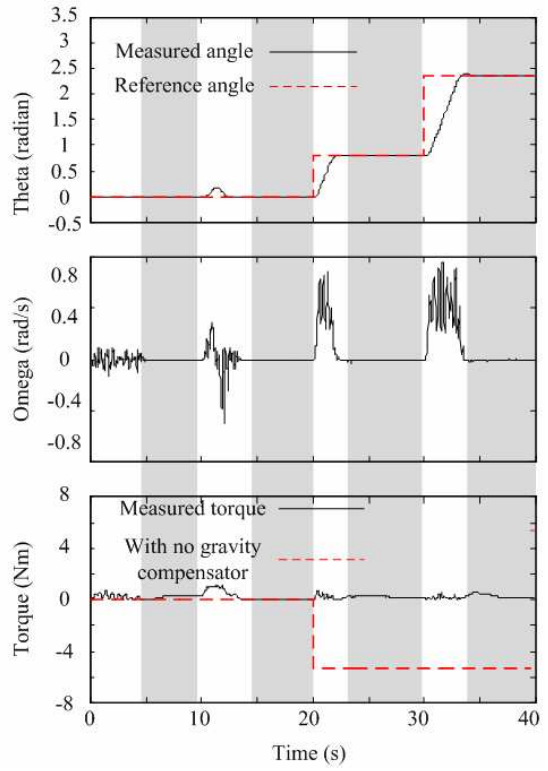

Fig. 5. The θ_1 experimental results.

torques with no gravity compensation, which are computed using $t_1 = mgls_1c_2$ and $t_2 = mglc_1s_2$ for the desired poses in Table 1. The static torques represent the desired motor torques needed to maintain the pose of the manipulator. The values of the measured torques are almost zero during omega ≅ 0 (i.e., the gray areas) for all instances, whereas those of the static torques are relatively large. These results indicate that gravity compensation was effectively achieved in half of the hemispherical work space.

It is noted that the measured torques should have zero values in the ideal situation. In practical situations, however, the measured torques have non-zero values because of joint friction. Friction provides the gravity compensator with certain torque margins. That is, a manipulator can hold its pose even when gravity compensators generate inaccurate torques. Since low 38:1 reduction ratios were adopted in the experiment to minimize the effect of the gear friction torque, the manipulator becomes fully backdrivable as in a haptic device. Therefore, it can be assumed that narrow torque margins were provided in the experiments. However, we could not accurately measure

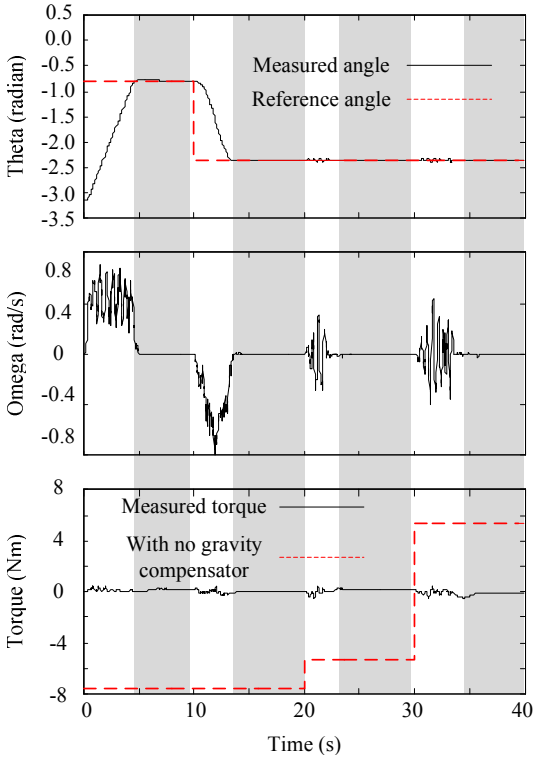

Fig. 6. The θ_2 experimental results.

or estimate the friction torque or the torque margin, since no torque sensors were implemented into the manipulator.

5. Conclusions

This paper presents a 2-dofs gravity compensator for roll-pitch rotations in which a bevel differential and two 1-dof gravity compensators are implemented. The spring coefficient was determined that achieved complete gravity compensation. The experiment results show that the bevel gravity compensator can effectively counterbalance the gravitational torques and can be operated in a hemispherical work space. From the various experiments, the following conclusions are drawn:

(1) The roll-pitch rotations are effectively decoupled by the bevel differential to provide a hemispherical work space.

(2) Complete gravity compensation is achieved with two 1-dof gravity compensators implemented at the decoupled rotations.

(3) Half of the stiffness needed for a 1-dof gravity compensator is necessary for the bevel gravity compensator.

In future studies, it will be necessary to investigate the adaptation to a payload, since the effects of the payload are critical to gravitational torques.

Acknowledgment

This research was supported by the MKE (The Ministry of Knowledge Economy), Korea, under the ITRC (Information

Technology Research Center) support program supervised by the NIPA (National IT Industry Promotion Agency)(NIPA-2012-H0301-12-2008).

References

[1] H. Diken, Effect of mass balancing on the actuator torques of a manipulator, *Mech. and Mach. Theory*, 30 (4) (1995) 495-500.

[2] Q. Lu, C. Ortega and O. Ma, Passive gravity compensation mechanisms: Technologies and applications, *Recent Patents on Engineering*, 5 (1) (2011) 32-44.

[3] R. H. Nathan, A constant force generation mechanism, *ASME Journal of Mechanisms, Transmissions, and Automation in Design*, 107 (4) (1985) 508-512.

[4] N. Ulrich and V. Kumar, Passive mechanical gravity compensation for robot manipulator, *Proc. of the 1991 IEEE Int. Conf. on Robotics and Automation*, Sacramento, USA. (1991) 1536-1541.

[5] K. Koser, A cam mechanism for gravity-balancing, *Mechanics Research Communications*, 36 (4) (2009) 523-530.

[6] T. Morita, F. Kuribara, Y. Shiozawa and S. Sugano, A novel mechanism design for gravity compensation in three dimensional space, *Proc. of the 2003 IEEE/ASME Int. Conf. on Advanced Intelligent Mechatronics*, Kobe, Japan (2003) 163-168.

[7] G. J. Walsh, D. A. Streit and B. J. Gilmore, Spatial spring equilibrator theory, *Mechanism and Machine Theory*, 26 (2) (1991) 155-170.

[8] Y. Ono and T. Morita, An underactuated manipulation method using a mechanical gravity canceller, *J. Rob. Mechatron*, 16 (6) (2004) 563-569.

[9] K. A. Wyrobek, E. H. Berger, H. F. M. V. Loos and J. K. Salisbury, Towards a personal robotics development platform: Rationale and design of an intrinsically safe personal robot, *Proc. of the 2008 IEEE Int. Conf. on Robotics and Automation*, Pasadena, USA. (2008) 2165-2170.

[10] S. K. Agrawal and A. Fattah, Gravity-balancing of spatial robotic manipulators, *Mechanism and Machine Theory*, 39 (12) (2004) 1331-1344.

[11] C. M. Gosselin and J. Wang, On the design of gravity-compensated six-degree-of-freedom parallel mechanisms, *Proc. of the 1998 IEEE Int. Conf. on Robotics and Automation*, Leuven, Belgium (1998) 2287-2294.

[12] A. Russo, R. Sinatra and F. Xi, Static balancing of parallel robots, *Mechanism and Machine Theory*, 40 (2) (2005) 191-202.

[13] C. H. Cho, W. S. Lee and S. C. Kang, Static balancing of a manipulator with hemispherical work space, *Proc. of the 2010 IEEE/ASME Int. Conf. on Advanced Intelligent Mechatronics*, Montreal, Canada (2010) 1269-1274.

[14] C. H. Cho and S. C. Kang, Design of a static balancing mechanism with unit gravity compensators, *Proc. Of the 2011 IEEE/RSJ Int. Conf. on Intelligent Robots and Systems*, San franciso, USA (2011) 1857-1862.

Changhyun Cho received the B.S. and M.S. degrees in Mechanical Engineering from Kyunghee University, Korea, in 1997 and 1999, respectively and Ph.D. degree in Mechanical Engineering from Korea University, Korea, in 2005. He was with the Center for Intelligent Robotics, Frontier 21 Program at KIST from 2005 to Aug. 2008. He joined the faculty of Dept. of Control, Instruments, and Robot, Chosun University, Kwangju, Korea in 2008, where he has been an Assistant Professor since 2008. His current research interests are in the fields of mechanism design and control of robotic systems.

Woosub Lee received the B.S. degree in Mechanical Engineering from Sogang University in 1999 and the MS degree in Electronic Engineering from Yonsei University in 2004. He had been working as a Research Scientist at the Korea Institute of Science and Technology from 2004 until 2010. Since 2010, he is a Doctoral fellow in Dept. of Mechanical and Aerospace Engineering at Tokyo Institute of Technology His current research interests are the design and control of field robot system, and dependable manipulator.

Jinyi Lee received the B.S. degrees in Mechanical Design from Chonbuk University, Korea, in 1992 and the M.S. and Ph.D degree in Mechanical and Aeronautics & Space Engineering from Tohoku University, Sendai, Japan, in 1995 and 1998, respectively. He was a researcher from 1998 to 2000 with the Tohoku University, Iwate University, Iwate Techno-Foundation and Saitama University, Japan. From 2000 to 2003, he worked for Lacomm Co., Ltd. and Gloria Techniques, Korea, as a researcher. In 2003, he was an instructor with the Chosun University, Gwangju, Korea. Since 2009, he has been an Associate Professor Chosun university. His research interests are in application of magneto-optical film, laser and CCD line scan sensor, development of magnetic camera, mechatronic systems.

Sungchul Kang received the B.S., M.S. and Ph.D. degree in Mechanical Engineering from Seoul National University, Korea in 1989, 1991 and 1998 respectively. In 1991, he joined Korea Institute of Science and Technology. He was a one year postdoctoral researcher at the Mechanical Engineering Laboratory in 2000, Japan and visiting researcher at artificial intelligence laboratory of Stanford University, USA in 2006. Now he is a principal research scientist at KIST. His research interests include robot manipulation, haptic sensing and display, and field robot systems.